AD-A104 002 CALIFORNIA UNIV BERKELEY LAWRENCE BERKELEY LAB F/G 20/7
INTERACTION POTENTIALS FOR BR(2P) + AR, KR, XE (1S) BY THE CROS--ETC(U)
MAR 81 P CASAVECCHIA, G HE, R K SPARKS N00014-77-C-0101
UNCLASSIFIED LBL-11907 NL

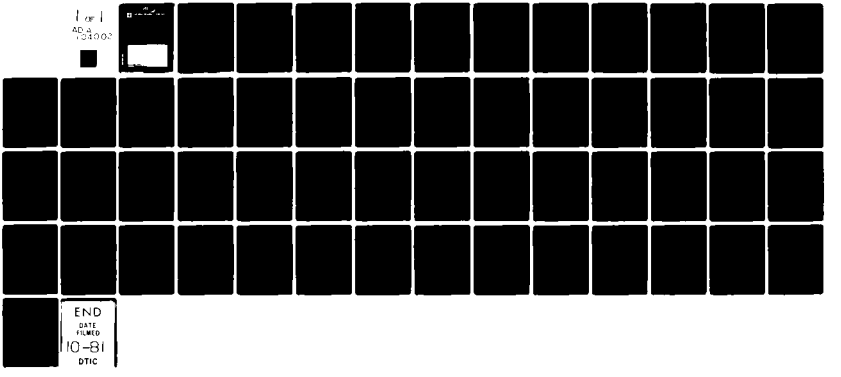

END
DATE FILMED
10-81
DTIC

Lawrence Berkeley Laboratory
UNIVERSITY OF CALIFORNIA

Materials & Molecular
Research Division

Submitted to the Journal of Chemical Physics

INTERACTION POTENTIALS FOR Br(^{2}P) + Ar, Kr, Xe (^{1}S) BY THE CROSSED MOLECULAR BEAMS METHOD

Piergiorgio Casavecchia, Guozhong He,
Randal K. Sparks, and Yuan T. Lee

Contract N00014-77-C-0101

March 1981

Prepared for the U.S. Departme

SECURITY CLASSIFICATION OF THIS PAGE (When Data Entered)

REPORT DOCUMENTATION PAGE

READ INSTRUCTIONS BEFORE COMPLETING FORM

(14) LBL-11907, UC-77-C-0101-1

1. REPORT NUMBER

2. GOVT ACCESSION NO. AD-A104002

3. RECIPIENT'S CATALOG NUMBER

4. TITLE (and Subtitle)

(6) INTERACTION POTENTIALS FOR Br(^{2}P) + Ar, Kr, Xe (^{1}S) BY THE CROSSED MOLECULAR BEAMS METHOD

5. TYPE OF REPORT & PERIOD COVERED

(9) Interim rept.,

6. PERFORMING ORG. REPORT NUMBER

LBL-11907

7. AUTHOR(s)

(10) Piergiorgio Casavecchia, Guozhong He, Randal K. Sparks, and Yuan T. Lee

8. CONTRACT OR GRANT NUMBER(s)

(15) N00014-77-C-0101, W-7405-eng-48

9. PERFORMING ORGANIZATION NAME AND ADDRESS

Materials & Molecular Research Division, Lawrence Berkeley Laboratory and Department of Chemistry, Univ. of Calif., Berkeley

10. PROGRAM ELEMENT, PROJECT, TASK AREA & WORK UNIT NUMBERS

12) 54

11. CONTROLLING OFFICE NAME AND ADDRESS

(11) Office of Naval Research
Washington, D.C.

12. REPORT DATE

March 1981

13. NUMBER OF PAGES

48

14. MONITORING AGENCY NAME & ADDRESS (if different from Controlling Office)

15. SECURITY CLASS. (of this report)

15a. DECLASSIFICATION/DOWNGRADING SCHEDULE

16. DISTRIBUTION STATEMENT (of this Report)

Unrestricted

DISTRIBUTION STATEMENT A
Approved for public release;
Distribution unlimited

17. DISTRIBUTION STATEMENT (of the abstract entered in Block 20, if different from Report)

18. SUPPLEMENTARY NOTES

19. KEY WORDS (Continue on reverse side if necessary and identify by block number)

Interaction potentials between rare gas atoms with bromine atoms investigated by crossed molecular beam scattering experiments.

20. ABSTRACT (Continue on reverse side if necessary and identify by block number)

Angular distributions of Br($^2P_{3/2,1/2}$) scattered off Ar, Kr, and Xe ($^1S_0$) in the thermal energy range measured in crossed molecular beams experiments. Interaction potentials for the $X\frac{1}{2}$ and $I\frac{3}{2}$ states are derived by using an approximate elastic scattering analysis, which neglects interstate coupling, as previously done for F-Xe, Kr, Ar, Ne and Cl-Xe. While the Br-Xe $X\frac{1}{2}$ potential (ε = 0.645 kcal/mole, r_m = 3.80 Å) shows a stronger

DD FORM 1 JAN 73 1473 EDITION OF 1 NOV 65 IS OBSOLETE
S/N 0102-LF-014-6601

407799 xlt

SECURITY CLASSIFICATION OF THIS PAGE (When Data Entered)

interaction than the interaction potential of Kr-Xe, the Br-Kr (ϵ = 0.460 kcal/mole, r_m = 3.90 Å) and Br-Ar (ϵ = 0.380 kcal/mole, r_m = 3.73 Å) $X\frac{1}{2}$ potentials are closer to those of the corresponding rare gas pairs. The $I\frac{3}{2}$ potential for all three systems is found to have a shallower ϵ, a slightly larger r_m and a more repulsive wall than the $^1\Sigma^+$ potential of the corresponding rare gas pair. The origin of these interactions is discussed and an attempt to examine the rare gas halides ground state bonding is presented.

LBL 11907

INTERACTION POTENTIALS FOR Br(^{2}P) + Ar, Kr, Xe (^{1}S) BY THE CROSSED MOLECULAR BEAMS METHOD

Piergiorgio Casavecchia,[a] Guozhong He,[b]
Randal K. Sparks,[c] and Yuan T. Lee

Materials and Molecular Research Division
Lawrence Berkeley Laboratory
and
Department of Chemistry
University of California
Berkeley, California 94720

ABSTRACT

Angular distributions of Br($^2P_{3/2,1/2}$) scattered off Ar, Kr, and Xe ($^1S_0$) in the thermal energy range were measured in crossed molecular beams experiments. Interaction potentials for the $X\frac{1}{2}$ and $I\frac{3}{2}$ states are derived by using an approximate elastic scattering analysis, which neglects interstate coupling, as previously done for F-Xe,Kr,Ar,Ne and Cl-Xe. While the Br-Xe $X\frac{1}{2}$ potential (ϵ = 0.645 kcal/mole, r_m = 3.80 Å) shows a stronger interaction than the interaction potential of Kr-Xe, the Br-Kr (ϵ = 0.460 kcal/mole, r_m = 3.90 Å) and Br-Ar (ϵ = 0.380 kcal/mole, r_m = 3.73 Å) $X\frac{1}{2}$ potentials are closer to those of the corresponding rare gas pairs.

---

a Permanent address: Dipartimento di Chimica dell'Universita, 06100 Perugia, Italy.
b Permanent address: Institute of Chemical Physics, Darien, People's Republic of China.
c Permanent address: Division of Chemistry and Chemical Engineering, California Institute of Technology, Pasadena, CA 91125.

The $I\frac{3}{2}$ potential for all three systems is found to have a shallower ϵ, a slightly larger r_m and a more repulsive wall than the $^1\Sigma^+$ potential of the corresponding rare gas pair. The origin of these interactions is discussed and an attempt to examine the rare gas halides ground state bonding is presented.

I. INTRODUCTION

Following the discovery of UV emission from rare gas monohalide molecules (RG-X)[1] and their subsequent use in high power UV lasers,[2] much work has been devoted to the spectroscopy and kinetics of these systems. The electronically excited RG-X systems have strong chemical interactions, ionic in character, quite similar to those of ground state alkali halides and have been studied extensively in both theoretical[3] and experimental investigations.[1b-d,4,5]

The picture of the interaction potentials of ground state RG-X is still not complete. In many systems, especially those involving light rare gas atoms and heavy halogen atoms, the interactions are expected to be rather weak and similar to van der Waals interactions between two rare gas atoms. On the other hand, interactions stronger than ordinary van der Waals forces recently have been shown to exist in systems such as XeF[6-8] and XeCl.[9,10] Since, with the exception of these two compounds, all of the observed emission spectra of the RG-X show only the diffuse structure characteristic of a bound-free transition, only very limited information on the ground state potential energy surfaces is obtained from these spectra.

The properties of the RG-X have also been the subject of intensive theoretical investigation.[11] Ab initio calculations have been reported on the covalent and ionic states of NeF, ArF, KrF, XeF[3a] and XeCl, XeBr, XeI[3b] by Dunning and Hay. An important role of these calculations has been to provide a detailed assignment of all of the features in the emission spectra of the RG-X and to predict previously

unobserved features. However, a slight rearrangement in the ordering of the excited $II\frac{3}{2}$ and $III\frac{1}{2}$ states was found to be necessary from the very recent detailed experimental investigations.[12] In contrast to the useful information obtained for the excited states from ab initio calculations, very little reliable information has been obtained to date on the ground state interaction. However, it is known that standard quantum chemical computational methods, even of CI type, usually fail for van der Waals type interactions.[13]

The crossed molecular beams technique has proven to be a powerful tool to give quantitative information on many adiabatic potentials not readily accessible to spectroscopic investigation.[14] The extraction of interaction potentials from scattering data for systems containing non-S state open shell atoms, such as halogen (^2P) or oxygen (^3P) with rare gas atoms, is complicated by the fact that there is more than one potential energy surface involved. Nevertheless, it is possible to obtain meaningful results if differential cross sections are carefully measured at several collision energies covering a wide angular range, and if the nonadiabatic coupling between the relevant states is weak. Accurate potentials in the well region for F-Xe $X\frac{1}{2}$ [8] and Cl-Xe $X\frac{1}{2}$ [10] have been obtained in this laboratory from differential cross section measurements, and are in very good agreement with spectroscopically determined potentials.[6,7,9] Also, molecular beam experiments have provided, for the first time, information on the F-Xe[8] and Cl-Xe[10] $I\frac{3}{2}$ and $II\frac{1}{2}$ potentials in the attractive well region. These potentials are inaccessible to spectroscopic study. The $X\frac{1}{2}$, $I\frac{3}{2}$ and $II\frac{1}{2}$ potentials have also been obtained for F-Ne, F-Ar and F-Kr.[15]

Br-Xe was the first rare gas halide system in which laser action (at 282 nm) was achieved.[2a] Only spontaneous emission has been reported for the Br-Kr[4,16] and Br-Ar systems.[16] Recently, from the analysis of emission spectra of Br-Ar at low pressure,[17] the positions and the slopes of the repulsive part of the $X\frac{1}{2}$ and $I\frac{3}{2}$ potential curves in the Frank-Condon region have been obtained, relative to the predetermined upper state potentials. Similar information is also available for the repulsive part of the Br-Xe $X\frac{1}{2}$ potential,[18] but the spectroscopic analysis has not been reported yet for Br-Kr.

In the past, the theoretical understanding of the termolecular recombination of bromine atoms in the presence of a inert gas as third body[19-21] has suffered from the lack of detailed information on Br-RG interaction potentials. Knowledge of the ground state potential in RG-X systems is also important in terms of fundamental bonding theory, especially, the transition from van der Waals interaction to chemical forces. Hence, in an attempt to better understand the RG-X ground state interaction in the attractive well region, and to provide useful information pertinent to RG-Br laser and recombination studies, we have measured the differential cross sections of $Br(^2P)$ scattered off Ar, Kr and $Xe(^1S)$ in the thermal energy range. The study reported here is a continuation of previous investigations from this laboratory on F-Ne, Ar, Kr, Xe[8,15] and Cl-Xe.[10]

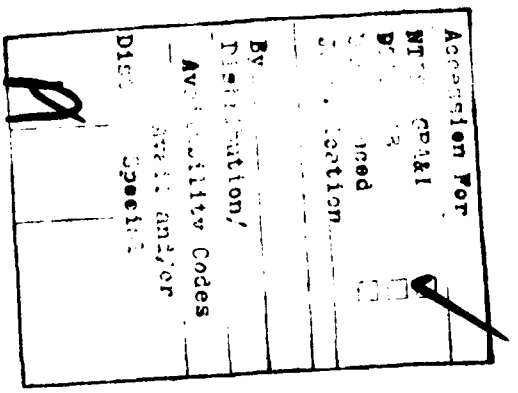

II. EXPERIMENTAL

The crossed molecular beams apparatus employed in this study is a newly designed higher resolution version[22] of the universal crossed molecular beam machine described by Lee et al.[23] Supersonic beam of bromine atoms seeded in a rare gas carrier, and beams of argon, krypton or xenon are crossed at 90° in a liquid nitrogen cooled collision chamber maintained at 8×10^{-8} torr. Elastically scattered bromine atoms are detected in the plane defined by the two intersecting beams, by a triply differentially pumped rotatable ultra high vacuum quadrupole mass spectrometer detector. The laboratory scattering angle, Θ, is measured relative to the Br beam direction.

The high intensity supersonic atomic bromine beams used in this study are produced in a resistance heated graphite nozzle which has been described in detail elsewhere.[24] The collision energy, E, was varied by changing the carrier gas while keeping the nozzle temperature at ~1800 K. Three different seeded mixtures were generated by passing pure xenon, argon or helium through a reservoir containing liquide bromine kept at 0°C. The heated gases expand through a 0.10 mm orifice at the tip of the oven. A 0.94 mm diameter graphite skimmer was used with a nozzle-skimmer distance of 8.5 mm. The beam was collimated in a differential pumping region to an angular spread of 1.0°. The rare gas beam expanded through a 0.07 mm quartz nozzle at room temperature and was collimated to an angular divergence of 1.9°. The nozzle-skimmer distance was 5.6 mm and the skimmer diameter 0.64 mm. Under our geometrical arrangement the collision volume is always contained in the viewing angle of the detector, which has an angular resolution

of 1.0°. The velocity distributions of the beams are characterized by conventional "single shot" time-of-flight (TOF) measurements with a 30 cm flight path from the slotted disc to the ionizer. Table I gives the Br, Ar, Kr and Xe atom effective bulk flow temperature, stagnation pressure, Mach number, peak velocity and full-width-half-maximum (FWHM) relative velocity spread. The most probable collision energy for each condition is also presented. Velocity distributions of the Br seeded beams are shown in Fig. 1. The solid line is a parametric fit to the deconvoluted distribution for the Mach number and the temperature given in Table I. The performance of the graphite oven as a source of bromine atoms has been excellent, showing stability and reproducibility even after a long period (~two months) of daily operation.

Laboratory angular distributions, $I(\textcircled{H})$, were obtained by taking from 4 to 6 scans of 20 sec. counts at each angle. Typically, signal at m/e 81 was detected. The $I(\textcircled{H})$ are time normalized by periodically returning the detector to an arbitrary reference angle (usually 10°) in order to account for possible long term drifts in beam intensities and detector sensitivity. The rare gas target beam was modulated at 150 Hz by a tuning fork chopper. Signal plus background and background counts were obtained from a pulse counting dual scaler, synchronously gated with the tuning fork.

The graphite nozzle temperature has been estimated based on the effective temperature of the gas in the nozzle. This temperature scale is determined from analysis of the measured TOF distributions of pure helium beams produced by expansion from the graphite nozzle at several different values of the heating power (a reference thermocouple was

placed close to the tip of the nozzle). Under the normal operating temperature (~1800 K) a small fraction of the spin-orbit (S-O) excited Br $^2P_{1/2}$ atoms is produced. Because of the large S-O splitting (3685 cm^{-1}), the amount of electronic to translational relaxation during the supersonic expansion is expected to be very small. Thus, the Br($^2P_{1/2}$) contribution to the beam is estimated by Boltzmann distribution and degeneracy weight to be 2.6 percent. Some small amount of undissociated bromine was also present in the beam and the small (a few percent) $^{81}Br^+$ contribution from Br_2 was taken into account from the measured angular distribution of Br_2 detected as $^{162}Br_2^+$ and the fragmentation ratio of Br_2, $^{81}Br^+/^{162}Br_2^+$ in the ionizer. This was then subtracted from the laboratory angular distribution measured at $^{81}Br^+$ to give the final I(Ⓗ) of Br+RG. In order to determine the Br_2 fragmentation ratio, the $^{81}Br^+/^{162}Br_2^+$ ratio for the ionization of Br_2 was measured as a function of oven temperature in a temperature range where negligible dissociation takes place. Almost constant values were obtained and then extrapolated to the operation temperature. A similar procedure was used satisfactorily during previous studies on F-RG[8,15] and Cl-Xe.[10]

Electronic transitions are expected to occur with very small cross sections in Br(^2P_J)+RG($^1S_0$) collisions[25] in the investigated energy range, because of the large S-O splitting of the Br doublet. Thus, a negligible contribution to the measured I(Ⓗ) is expected from inelastic events. As a consequence, no attempt was made to investigate the fine structure inelastic transitions by TOF measurements.

III. RESULTS AND ANALYSIS

Laboratory angular distributions $I(\textcircled{H})$ of Br scattered off Xe, Kr and Ar are presented on a semi-log scale in Figs. 2, 3 and 4, respectively. Exemplary error bars are shown, when visible outside the solid circle, representing ±2 standard deviations of the mean. The nominal collision energies, E, are also indicated. While $^{81}Br^+$ was detected in the Br+Ar and Xe experiments, $^{79}Br^+$ was detected in the Br+Kr case, in order to avoid interference from the possible transmission of a small amount of $^{82}Kr^+$ at m/e = 81 coming from the elastically scattered krypton beam.

The $I(\textcircled{H})$ for Br-Xe (see Fig. 2) at E=4.2 kcal/mole clearly shows a low amplitude rainbow structure. A significant portion of rainbow on the dark side is seen at E=9.8 kcal/mole, while at the highest E the distribution mainly reflects the scattering from the repulsive parts of the potentials.

The $I(\textcircled{H})$ for Br-Kr (see Fig. 3) at E=3.8 kcal/mole shows a rainbow structure at small angles, while at E=8.4 kcal/mole only the dark side of the rainbow scattering is observed.

The rainbow structure is barely seen for Br-Ar at E=2.9 kcal/mole shown in Fig. 4. A slower Br beam would have been desirable in order to obtain a significantly lower collision energy and consequently shift the rainbow oscillation to larger angles. Unfortunately, the nozzle temperature cannot be decreased without a drastic reduction of Br_2 dissociation. Also, Br_2 was already seeded in the heaviest rare gas, Xe. The unusual shape of the $I(\textcircled{H})$ at large angles for Br-Ar, particularly pronounced at high E, is due to the detection of heavier

atoms in this system. When one detects the heavy particle, particles scattered at two different center-of-mass (CM) angles are observed at the same laboratory angle. The heavier bromine atom is kinematically constrained to scatter within a lab angle of approximately 38° at E=14.8 kcal/mole and of approximately 55° at E=2.9 kcal/mole, as predicted from the most probable Newton diagrams. As we approach the edge of the elastic Newton circle, the differential cross section shows a rather broad peak in the vicinity of these cutoff angles due to the nature of the transformation Jacobian which relates the lab and CM reference frames.[14] The angular distributions shown in Fig. 4 have been truncated at large angles near the onset of this peak. This effect has been properly accounted for in the data analysis.

The procedure of analysis to obtain interaction potentials for the states involved in the scattering by fitting the I(Ⓗ) is the same as that of Refs. 8, 10 and 15 and will only be briefly discussed here. The molecular electronic states arising from the four-fold degenerate ground state $Br(^2P_{3/2})$ + $RG(^1S_0)$ asymptote are the doubly degenerate $X\frac{1}{2}$ (or $I\frac{1}{2}$) and $I\frac{3}{2}$ states, in Hund's case c notation. (In Hund's case b and a notation these are designated $^2\Sigma^+_{1/2}$ and $^2\Pi_{3/2}$, respectively). From the doubly degenerate spin-orbit excited manifold, $^2P_{1/2}$ + $^1S_0$, one obtains the $II\frac{1}{2}$ state ($^2\Pi_{1/2}$ in Hund's case a). In this notation the 1/2 or 3/2 represents the Ω quantum number (the projection of the total electronic angular momentum along the internuclear axis); the X, I, II represents the ordering of the states.

It has been shown that inelastic cross sections are much smaller than the elastic cross sections for F-Ar, Xe and Cl-Xe in the thermal

energy range.[25] Since the inelastic cross sections should be even smaller for the Br-RG systems, the total differential cross section can be written as a sum of elastic differential cross sections ${}^{\sigma}X_{1/2}(\theta)$, ${}^{\sigma}I_{3/2}(\theta)$, and ${}^{\sigma}II_{1/2}(\theta)$ for the three states X 1/2, I 3/2 and II 1/2. Each state's contribution is given its appropriate statistical weight and added to give a total $\sigma_T(\theta)$:

$$\sigma_T(\theta) = \frac{1}{2}(0.974)\left[\sigma_{X\ 1/2}(\theta) + \sigma_{I\ 3/2}(\theta)\right] + (0.026)\sigma_{II\ 1/2}(\theta)$$

$$\simeq 0.487\ \sigma_{X\ 1/2}(\theta) + 0.513\ \sigma_{I\ 3/2}(\theta) \qquad (1)$$

The approximation $\sigma_{II\ 1/2} \simeq \sigma_{I\ 3/2}$ has been used. Because of the small contribution of $\sigma_{II\ 1/2}$ to σ_T, this approximation should have a negligible effect in the evaluation of the $V_{X\ 1/2}(r)$ and $V_{I\ 3/2}(r)$. Each elastic differential cross section in the CM system is calculated independently by partial wave analysis with JWKB phase shifts[26] to give a calculated I(Ⓗ) with appropriate averaging over the velocity and angular distributions of the two beams and the detector acceptance angle. Comparison of calculated I(Ⓗ) with experimental I(Ⓗ) provides the basis for evaluation of the interaction potentials.

The accuracy of this case c elastic approximation has been supported in two ways as shown in previous studies.[8,10,15] First, in the F-Xe case, where an accurate spectroscopically (RKR) determined potential was available,[6,7] for the $V_{X\ 1/2}(r)$ this scattering method was found to give results in good agreement.[8] Scattering studies[10] were also fruitful in corroborating a spectroscopically obtained

$V_{X\ 1/2}(r)$ for Cl-Xe.[9] Second, rigorous coupled-channel scattering computations[25] show that the elastic approximation reproduces all of the gross features of the experimental $I(\textcircled{H})$ very well for F-Xe, F-Ar and Cl-Xe at thermal energies. The approximation is expected to hold even better for systems where the open shell atom has larger S-O splitting, such as bromine and iodine.

The physical meaning of the elastic analysis used here is that the electron orbital and spin angular momentum remain coupled throughout the collision and coupling is weak between the adiabatic states of the total electronic Hamiltonian including S-O interaction. Hund's case c affords a good description of this situation, with Ω being the good quantum number.[27,28] This model corresponds to describing the collisions by elastic scattering separately on each of the adiabatic potential energy curves. The same model has been followed by Aquilanti et al.[29] in the analysis of their results on the scattering of magnetically selected $O(^3P)$ atoms with rare gases at thermal energies; absolute integral cross sections were measured. Our model is physically very different from the elastic models (see Ref. 30 and references cited therein) previously used to describe thermal collision of systems with small S-O coupling, such as $Li(^2P)$-RG. Those models are based on the assumption that, during the collision, the electron orbital angular momentum and spin remain uncoupled, and that coupling is weak between the adiabatic states of the electrostatic electronic Hamiltonian.

In the analysis of the experimental results of Figs. 2, 3 and 4, the interaction potentials V(r) are chosen to be the flexible, piecewise analytic, Morse-Morse-switching function-van der Waals (MMSV) form. The MMSV reduced form is given by:

$$f(x) = V(r)/\epsilon \qquad x = r/r_m$$

$$f(x) = \exp(2\beta_1(1 - x)) - 2\exp(\beta_1(1-x)) , \qquad 0<x\leq 1$$

$$= \exp(2\beta_2(1 - x)) - 2\exp(\beta_2(1 - x)) \equiv M_2(x) \qquad 1<x\leq x_1$$

$$= SW(x)\, M_2(x) + (1 - SW(x))\, W(x) \qquad x_1<x<x_2$$

$$= -C_{6r}x^{-6} - C_{8r}x^{-8} \equiv W(x) \qquad x_2\leq x<\infty$$

and

$$SW(x) = \frac{1}{2}\left[\cos\frac{\pi(x - x_1)}{(x_2 - x_1)} + 1\right] ,$$

where

$$C_{6r} = \frac{C_6}{(\epsilon r_m^6)} \text{ , and } C_{8r} = \frac{C_8}{(\epsilon r_m^8)} \text{ ;}$$

ϵ and r_m are the depth and position of potential minimum.

The van der Waals C_6 constant is estimated by the Slater-Kirkwood formula[31] for effective number of electrons:

$$C_6 = \frac{3}{2}\frac{\alpha(Br)\ \alpha(RG)}{[\alpha(Br)/N(Br)]^{1/2} + [\alpha(RG)/N(RG)]^{1/2}}$$

where $\alpha(Br)$ and $\alpha(RG)$ are the polarizabilities of bromine atoms[32] and rare gas atoms (RG=Ar, Kr, Xe),[33] respectively, and N is the effective number of electrons [N(Br)=5.7, N(Ar)=6.0, N(Kr)=6.7 and N(Xe)=7.93]. The halogen atoms are known to have an anisotropy of polarizability, being $\alpha(m_j=\pm 1) > \alpha(m_j=0)$.[34,35] The anisotropy of Br, for which no experimental or theoretical value was found, has been

taken to be equal to that of Cl (~15%),[35] which is slightly larger than that of F (~12%).[34] The C_6 constant of I 3/2 is calculated to be larger than X 1/2 state, reflecting the larger polarizability of the Π symmetry. This implies a slow curve crossing for the X 1/2 and I 3/2 states at fairly large r, as obtained for the F-RG and Cl-Xe. The C_6 for the X 1/2 state has the long range mixture of one-third $^2\Pi$ and two-thirds $^2\Sigma^+$ character,[3a-b,36] while I 3/2 is purely $^2\Pi$. The II 1/2 state asymptotically approaches two-thirds $^2\Pi$ and one-third $^2\Sigma^+$, but we have used the C_6 of the I 3/2 state, since we have assumed $V_{II\ 1/2} \simeq V_{I\ 3/2}$. This should have a negligible effect. The C_8 constants are estimated from the Kr-Rg (Rg=Ar,Kr,Xe) C_8 constants.[33] The permanent quadrupole induced dipole induction constant, varying as R^{-8} at long-range, contributes only a small fraction of the C_8 dispersion term, as estimated from the permanent quadrupole moment of Br^{37} and the polarizability of the rare gases.[33] It has thus been neglected, as have higher order constants, because of their uncertainty and very small contribution.

Initially, the I 3/2 potentials for all three systems were assumed to be very near the corresponding one electron richer rare gas pair Kr-RG. Justification of this choice is based on the closed shell-closed shell electronic configuration for the Π symmetry, having the fully occupied bromine p orbital along the internuclear axis.[3a] With this assumption the parameters ϵ, r_m, β_1, and β_2 for the X 1/2 potential were varied in an attempt to match the calculated and experimental I(Ⓗ) at three collision energies for Br-Xe and two collision energies for Br-Kr and Br-Ar. In order to reach a good simultaneous

fit in all the angular ranges, the original estimate of the I 3/2 potential needed to be slightly modified in the well depth for all three systems. In the Br-Ar case, r_m also needed to be modified. A little variation was also made in the x_1 and x_2 values for both potentials. The best fit I(Ⓗ) are reported as a solid line in Figs. 2, 3 and 4 for Br-Xe, Br-Kr and Br-Ar, respectively. The calculated I(Ⓗ) are scaled to the data by a constant scaling factor which is determined by the minimization of a chi(χ)-square goodness of fit measure. The derived $V_{X\ 1/2}(r)$ and $V_{I\ 3/2}(r)$ potentials are depicted in Figs. 5, 6 and 7. The resulting potential parameters are listed in Table II, where those of the Kr-Ar,[38] Kr-Kr[39] and Kr-Xe[40] systems are also reported for comparison. The contribution to I(Ⓗ) by each of the potentials reported in Table II is shown with discontinuous lines in Fig. 2 for Br-Xe at three energies and in Figs. 3 and 4 for Br-Kr and Br-Ar only at the lowest E. The relative weights from Eq. (1) are used in the I(Ⓗ) plot for all energies.

Measurements of I(Ⓗ) at more than one collision energy and covering a wide angular range allow an accurate estimate of the two interaction potentials which contribute most to the scattering. In fact, rainbow and supernumerary rainbow positions and relative intensities are very sensitive to potential well depths and curvature.[14,41] Also, the range parameters of the potentials are sensitive to the ratio of rainbow to wide angle scattering intensities. In particular, the relative magnitude of the cross section at large angles to that at the rainbows gives a good indication of the "size" of the atoms, that is, the position of the repulsive wall of the

potential. Quite strong sensitivity to the $V_{X\ 1/2}$ well of Br-Xe was found in the lowest energy angular distributions. As shown in Fig. 2 at E=4.2 kcal/mole, the main rainbow and the first supernumerary from the X 1/2 potential are observed (dashed line). The main rainbow produced by the I 3/2 potential is also clearly observed (dot-dashed line) providing quite good sensitivity of I(Ⓗ) also to the $V_{I\ 3/2}$. A pronounced quenching can be noted when the two separate contributions are added according to Eq. (1) to give the best fit I(Ⓗ); but, two major low amplitude oscillations can still be seen. At E=9.8 kcal/mole significant contribution from the $V_{X\ 1/2}$ rainbow is still observed. While at the highest E, the separated contributions clearly show that scattering is mainly taking place from the repulsive walls of the two potentials. The data presented in Fig. 2 allows an estimate of ϵ and r_m parameters for the $V_{X\ 1/2}(r)$ to within ±5 percent and for the $V_{I\ 3/2}(r)$ to within ±7 percent for Br-Xe. Estimates of the uncertainties were obtained by making a matrix of plots of computed I(Ⓗ), with the different matrix elements corresponding to potentials with differing (ϵ, r_m) values (always keeping the overall potentia's to a reasonable shape). The ϵ and r_m values were varied for the two different states until the fits to the experimental I(Ⓗ) became poor. These computations were made for every system at all the energies investigated. Possible error in the Morse β parameters are likely to be of similar magnitude, based on their observed influence on the I(Ⓗ) during the trial and error fitting procedure. Because the quality of the data at large angles are also quite good, fairly high sensitivity to the repulsive walls is obtained. Of course, these

potentials for Br-Xe can be considered valid on the repulsive wall only to about 26 kcal/mole, which is the highest collision energy studied.

Figure 3 shows that, for the Br-Kr system at E=3.8 kcal/mole, the main rainbow oscillation from both potentials is observed. Again, the total $I(\textcircled{H})$ is strongly quenched, particularly because the oscillatory behaviors of the two different rainbow patterns are out of phase. Figure 4 shows that the rainbow structure from the $V_{X\ 1/2}$ is almost fully resolved at E=2.9 kcal/mole for Br-Ar, while only a portion of the dark side of the rainbow from the $V_{I\ 3/2}$ is seen. For Br-Kr and Br-Ar, a slightly lower sensitivity of $I(\textcircled{H})$ to the ϵ and r_m parameters of the $V_{X\ 1/2}$ and $V_{I\ 3/2}$ than for Br-Xe is observed. The estimated maximum uncertainties in ϵ and r_m, obtained with the procedure described above, for both systems are within ± 7 percent and ± 10 percent for $V_{X\ 1/2}(r)$ and $V_{I\ 3/2}(r)$, respectively. Uncertainties for the Morse parameters, which govern the shape of the potentials near the minimum and the repulsive wall are similar to those obtained for ϵ and r_m.

We note that the final x_2 joining points obtained are slightly larger than the cut-off points $2\ [\langle r_{Br}^2\rangle^{1/2} + \langle r_{RG}^2\rangle^{1/2}]$ suggested[42] for the validity of the power series expansion, which were taken as initial guesses. The C_6 and C_8 van der Waals constants were kept fixed during the fitting, because the differential cross section is not very sensitive to the long range part of the potential. Consequently, no accurate information is gained on the long range van der Waals attraction.

IV. DISCUSSION

A detailed characterization of the bound-free emission spectra of the RG-X would require a knowledge of the potential energy curves of both the upper and lower states over the relevant range of energy and internuclear distance, in addition to the variation of the electronic transition moment with internuclear distance and the vibrational distribution of the emitting states. The close analogy of the excited RG-X with ground state alkali halides has provided the basis for the interpretation and the prediction of the emission spectra.[4] From trial and error semiclassical simulation of the diffuse spectra, information on the upper states and approximate shapes for the lower state potential curves in the Frank-Condon region have been obtained.[17,18] But, no unique potential curves can be derived from diffuse emission spectra alone. In fact, the form of a spectrum is determined principally by the relative shapes of the upper and lower potentials.

A. Br-Xe.

The Br-Xe emission spectrum has been studied by several groups.[4,5,1c] Crude estimates of the upper III 1/2 (B) state vibrational frequency, ω_e', were given. The most recent and detailed investigation was performed by Tellinghuisen et al.,[18] who attempted a quantitative analysis of the high pressure III 1/2 → X 1/2 (B → X) bands. The ratios of ω_e's and the dissociation energies, D_e's, between XeBr and CsBr are found to be 0.80 and 0.91, respectively. In general ω_e' and D_e' values are always smaller for the RG-X, than for alkali halides, in qualitative accord with the replacement of

the alkali ion by the larger and softer rare gas ion. But, no simple quantitative explanation for the trend observed along the series has been found. The R_e' value of 2.96 Å used for the III 1/2 state in the spectrum simulation[18] is 0.11 Å shorter than R_e' for CsBr[43] and is significantly shorter than the theoretically calculated value of 3.38 Å.[3b] The ground state X 1/2 potential curve was found to have an appreciable slope in the Frank-Condon region, $-(dV_{X\ 1/2}/dR)_{R_e'}$ = 5.8±0.6 kcal/mole/Å.[18] The absolute $V_{X\ 1/2}(R_e')$ was estimated to be 1.4±0.6 kcal/mole. The repulsive wall of Br-Xe $V_{X\ 1/2}(r)$ obtained from the present study gives $-(dV_{X\ 1/2}/dR)R_e'=2.96$ Å$=5.6^{+1.9}_{-0.8}$kcal/moleÅ and $V_{X\ 1/2}(R_e')=1.0\pm0.3$ kcal/mole (see Fig. 5 and Table II). These appear to be in good accord with the spectroscopic estimates.[18] Thus, our results also represent indirectly a corroboration of the estimate of Tellinghuisen et al.[18] of the shape and position of the upper state potential, in addition to providing a more complete picture of $V_{X\ 1/2}(r)$ and $V_{I\ 3/2}(r)$. Because of the large S-O interaction in $Br(^2P)$ the non-ionic manifold should be clearly split into three distinct states.[3b] This produces important effects as far as the emission properties are concerned.[11] But, there appears to be no experimental observation as yet of the theoretically predicted band ending on the I 3/2 state. The III 1/2 → II 1/2 broad band has been investigated very recently.[44] The theoretical curves of Ref. 3b were used in an attempt to simulate the temperature dependence of the unstructured experimental spectra. Consequently, very little information exists on the $V_{I\ 3/2}(r)$ and $V_{II\ 1/2}(r)$. No direct information

is obtained about the latter from our study. However, in general, $V_{II\ 1/2}$ can be derived, as shown in Ref. 25, from the $V_{X\ 1/2}$ and $V_{I\ 3/2}$.

Our results for the Br-Xe system show that the $V_{X\ 1/2}(r)$ has a stronger interaction than the $V_X\ ^1\Sigma^+$ of Kr-Xe (see Table II).[40] The well depth is about 0.18 kcal/mole (~40 percent) deeper and r_m 0.32 Å shorter. Also, the Br-Xe inner wall appears to be much less repulsive. The higher polarizability of Br with respect to Kr cannot alone explain these effects. The binding energy of the X 1/2 state decreases in the sequence F-Xe, Cl-Xe and Br-Xe, probably in relation to the smaller electronegativity of the heavier halogens. In the F-Xe bonding[6-8,38] chemical forces seem to be operative; on the other hand, for Br-Xe, although the binding energy is closer to that of Kr-Xe, it does not seem to be entirely due to van der Waals interaction. The following contributions as a function of internuclear distance might provide the explanation of the $V_{X\ 1/2}(r)$ bonding in RG-X: (a) less repulsion due to an only half filled p orbital along the internuclear axis, (b) a certain amount of charge transfer further lessening this repulsion, and (c) the contribution from interatomic correlation energy (the dispersion energy in the limit of zero electron overlap). These arguments are used also by Krauss and Liu[45] to give a plausible explanation of the F-Xe $V_{X\ 1/2}(r)$. The S-O interaction was not included in their calculation, nor the variation of the intra-atomic correlation and the coupling between the inter- and intra-atomic correlation energy. The latter are difficult problems when one wishes to perform accurate computations.[46,13]

Hay and Dunning[3b] estimated the ionic contribution in configuration interaction (CI) to the X 1/2 state, at an interatomic distance which corresponds to the calculated R_e' of the ionic state. Ionic contribution was found to decrease modestly from F-Xe (9.4 percent) to Br-Xe (5.2 percent). The interaction between the covalent and ionic states provides a stabilizing ion-pair contribution to the X 1/2 state well depth, and a repulsive contribution to the III 1/2 curve. The results of our studies[8,10,15,47] appear to support a substantial charge-transfer in the X-Xe X 1/2 states, which does not seem to vary smoothly going from F-Xe to Br-Xe. As a consequence, the question of the accuracy of the CI calculations is raised. These calculations show the III 1/2 curve to lie above the II 3/2 curve only at internuclear distances shorter than R_e' of the III 1/2 excited state.[3a-b] However, recent experiments[12] have confirmed earlier indications[48] of a reversed ordering of the III 1/2 and II 3/2 states in xenon halides. The II 3/2 state is found to lie below the III 1/2 state by about 600 cm^{-1}, 128 cm^{-1} and 80 cm^{-1} in F-Xe, Cl-Xe and Br-Xe, respectively.[12] Krauss[3c] points out that the energy splitting between the ionic III 1/2 and II 3/2 curves is very dependent on the configuration mixing term between the ground X 1/2 state and the excited III 1/2 state. He notes also that the degree of mixing has little effect on the lifetime of the emitting states, which are indeed rather well predicted by the theory.[11] However, the possibility that CI calculations do not properly account for configuration interaction with the charge transfer state is also recognized by Hay and Dunning.[3b] From a comparison of calculated ω_e', D_e' and R_e'

with experimentally derived values, a fairly good agreement is observed between values of ω_e', while the calculated values of R_e' are systematically larger by 0.2-0.4 Å and the values of D_e' systematically lower.[11] The theoretical values were reasoned to be more reliable than the experimental R_e' values.[3b] However, the R_e' derived from experiments for the III 1/2 state of F-Xe[6,7] and Cl-Xe,[9] where rovibrational and vibrational structure, respectively, is resolved, are expected to be reliable. The results obtained for Br-Xe from our experiments also seem to confirm the "spectroscopic" value rather than theoretical calculations. The longer internuclear distance for ground state (X 1/2) relative to excited state (III 1/2) XeBr with respect to XeF and XeCl explains the lower absorption intensity for XeBr observed in spectroscopic studies of matrix-isolated XeF, XeCl and XeBr.[49]

While the Br-Xe $V_{X\ 1/2}$ clearly deviates from the corresponding Kr-Xe potential, as discussed above, the $V_{I\ 3/2}$ shows a close resemblance to it, being just 0.04 kcal/mole shallower and slightly more repulsive (see Table II). Since the polarizability of Br in the I 3/2 state of XeBr is higher than that of Kr in the Kr-Xe $X^1\Sigma^+$ state, the result has to be interpreted as a manifestation of a more repulsive character of the Π type interaction in the open shell-closed shell system, with respect to the Σ type closed shell-closed shell pure van der Waals interaction in the rare gas pair. This is due to the fully occupied p orbital along the molecular axis and the larger $\langle \bar{r}^2 \rangle$ of the outermost electron cloud of Br. The ionic-covalent configuration mixing is calculated to be much smaller for the I 3/2 state than

for the X 1/2 state.[3c] This is reflected in its significantly less bound character and in the smaller II 3/2 → I 3/2 transition moment.

The calculated X 1/2 and I 3/2 curves of Br-Xe are found to be essentially repulsive[3b] and consequently do not compare satisfactorily with the curves derived here. Nevertheless, ab initio calculations undoubtedly are of more value in describing the repulsive walls fairly far away from the region of the wells than are these scattering results, provided that the spin-orbit energy remains approximately constant with the internuclear distance.

B. Br-Kr,Ar

As can be seen from Table II, the results obtained for the Br-Kr and Br-Ar systems show that the well depth of the $V_{X\ 1/2}$ is only slightly deeper than those in the corresponding rare gas pairs, namely Kr-Kr[39] and Kr-Ar.[38] It seems that they begin to manifest a clear analogy to the rare gas pair. In fact, the slightly deeper ϵ (about 0.06 and 0.04 kcal/mole for Br-Kr and Br-Ar, respectively), and the modestly shorter r_m (about 0.1 Å for both systems) can be reasonably associated with the slight differences in the size of the outermost electron cloud between the bromine and krypton atoms and their polarizabilities anisotropic in the case of Br. Kr has a smaller radius for its outermost electrons since the Kr nucleus has one more nuclear charge than Br.[37] But Br has a larger polarizability than Kr, which will tend to offset the effects of the difference on atomic sizes. One should expect that in the X 1/2 state of Br-Kr and Br-Ar the bromine atom, having only one 4p electron on axis with the rare gas atom, could approach closer and the binding energy should be higher and the minimum position shorter than in Kr-Kr and Kr-Ar.

The experimentally derived I 3/2 potentials for Br-Kr and Br-Ar (see Table II and Figs. 6 and 7) have a larger r_m (by ~0.1 Å), a shallower ϵ (by about 0.05 and 0.08 kcal/mole for Br-Kr and Br-Ar, respectively), and are slightly more repulsive than the $X^1\Sigma^+$ potentials of Kr-Kr and Kr-Ar. A similar situation was observed also for the $V_{I\ 3/2}$ of Br-Xe, and as discussed in Sect. IV-A. The binding energy of the I 3/2 state of the rare gas bromides, being less than the rare gas-rare gas systems, indicate the larger Br outermost electron radius and the fully occupied p orbitals contribute to repulsion at larger values of internuclear separation.

Since Br has a larger polarizability than Kr, the short range repulsion seems to dominate the difference between $V_{X\ 1/2}$ and $V_{I\ 3/2}$ in the Br-RG (RG=Ar,Kr and Xe) diatomics. In an attempt to better understand the bonding, on the basis of our results we can try to estimate the relative contribution of the effect (i) of the outermost electron radius $\langle r^{-2} \rangle$, (ii) of the angular distribution of the outermost orbitals (i.e., half or fully occupied p orbital), and (iii) of the charge transfer. For the I 3/2 state we can neglect the effect of a poorly known contribution of charge transfer and the effect of the half-filled orbital. We can explain, then, the bonding of the I 3/2 state of the RG-Br to be mainly determined by the size of the outermost electron cloud of the halogen atom, when compared with the $X^1\Sigma^+$ state of the corresponding rare gas pair. This should also be valid for the I 3/2 state of the other RG-X. While for the X 1/2 state all the factors mentioned above give some contribution to the bonding. In this case, there is not sufficient information to allow us to distinguish

their relative contribution. However, we can gain some insight into this question on the basis of the following observations.

Going from Br-Xe to Br-Kr and Br-Ar, only changing the nature of the rare gas, two factors can explain the trend of the X 1/2 potentials: the more compact size and consequently lower polarizability of Kr and Ar with respect to Xe; and their higher ionization potential which pushes the energy of the ionic states higher. This last factor diminishes the degree of ionic-covalent mixing,[3c] which is one of the important contributing factors to the ground state X 1/2 binding energy. As can be seen from Figs. 5-7 and Table II, the X 1/2 state of Br-Xe has a deeper well and a significantly shorter r_m than Br-Kr and Br-Ar with respect to the $X'\Sigma^+$ state of the corresponding rare gas pair; it is also less repulsive. Hence, the repulsive walls of the X 1/2 and I 3/2 potentials are more clearly distinct in the Br-Xe case. The above observation suggests that the effect of charge-transfer may account for the differences in bonding along a specific halogen-RG series (i.e., Br-RG, Cl-RG, and F-RG, where RG = Xe,Kr, and Ar). The replacement of Xe with Kr or Ar was shown to have a dramatic effect on the rare gas monofluorides.[15] In this case the nature of the halogen, the strongly electronegative fluorine atom, also plays an important role in the anomalous trend within the series. In particular, the explanation of the almost chemical well in the X 1/2 state of F-Xe[6-8,15,45] should also depend critically on the contribution of the interatomic correlation energy. In fact, we note that when replacing F with Br, the relative positions of the covalent and ionic states of the separated atoms do not vary as much as when Ar is

replaced with Xe, since the rare gas ionization potentials vary over a much more extended range than the electron affinities of the halogen atoms. Since the $V_{X\ 1/2}$ well depth and equilibrium distance vary quite dramatically as we move from XeF (ϵ = 3.359 kcal/mole, r_m = 2.293 Å) through XeCl (ϵ = 0.80 kcal/mole, r_m 3.23 Å) to XeBr (ϵ = 0.645 kcal/mole, r_m = 3.80 Å), this seems to suggest that other factors in addition to the charge-transfer mixing play a significant role in a specific rare gas-X series (i.e., Xe-X, Kr-X, where X = F,Cl and Br). One of these factors may be the effect of the half occupied p orbital, "hard" in the small fluorine atom, "soft" in the large bromine atom. Another, very important factor,[45] is again the effect of the interatomic correlation energy. Now, from a comparison of F-Kr[15] with Br-Kr (or F-Ar[15] with Br-Ar) and F-Xe[8] with Br-Xe, we are lead to conclude that F-Xe is quite a "peculiar" system. It would seem that Xe is chemically more different from Kr or Ar, than F is from Cl or Br. It should be noted that in the F-Xe system we have a limiting situation: the smallest and most electronegative halogen atom with the most polarizable and consequently most easily ionizable rare gas atom. This situation may produce, as the result of several additive effects, a significant negative energy contribution. What we want to emphasize is that the presence of Xe is more critical than that of F, since, in the Kr-X or Ar-X (X=F, Cl, Br) series we don't observe such a "peculiar" system as F-Xe.

In the RG-X series the S-O interaction may also play an important role in the trends of the X 1/2 state bonding. Calculations show a dramatic increase in the admixture of Π character into the ground

X 1/2 state as one proceeds in the sequence XeF (0.045) XeCl (0.142), XeBr (0.379), and XeI (0.483).[3b] This should have a destabilizing effect on the X 1/2 state, because of the repulsive character of the I 3/2 and II 1/2 states. Such an effect can be expected to have the same importance in a specific halogen-RG series (RG=Ar,Kr and Xe). However, in their model Hay and Dunning neglect any interaction between covalent and ionic states in determining the S-O coupling elements. Little is known about the S-O interaction for open shell molecules. Other factors, such as the inclusion of a relativistic core and the influence of relaxing the restriction of the frozen Hartree-Fock core in Xe, have been shown to have negligible effect on calculated curves.[3b] Given that the different factors contributing to the bonding are to a good degree separable, the RG-X molecules may provide insight into the nature of interatomic correlation in regions of significant electron overlap.

It will be interesting to complete the series of the RG-X molecules, by studying also the RG-I systems.[50] It will then be possible to examine in a more complete fashion the effect of the halogen atom and/or of the rare gas atom on the potential energy curves of the RG-X.

No theoretical studies have been performed on the Br-Kr and Br-Ar systems. Recently, a systematic study of the Br-Ar emission spectra has been published by Golde and Kvaran.[17] By using spectroscopic and kinetic data, valuable information was obtained on the potential curves and vibrational distributions of the emitting states. Three partially overlapping transitions, ending on the three states of the lower Br-Ar

manifold, contribute to the continuum spectra, with obvious complication for the analysis. The upper III 1/2 and II 3/2 emitting states were predetermined by analogy with KBr and were taken to be essentially identical. The slopes and the absolute energy of the $V_{X\ 1/2}$ and $V_{I\ 3/2}$ in the Frank-Condon region were estimated. The most precise results were obtained for the $V_{X\ 1/2}$ from the analysis of the highly structured III 1/2 → X 1/2 continuum. The following estimate was determined:

$$-(dV_{X\ 1/2}/dR)_{R_e' = 3.09\ \text{Å}} = 13.1 \text{ kcal/(mole Å) and}$$

$V_{X\ 1/2}\ (R_e' = 3.09\ \text{Å}) = 4.6$ kcal/mole, with an uncertainty of about 10 percent. Our best fit results give:

$$-(dV_{X\ 1/2}/dR)_{R_e' = 3.09\ \text{Å}} \cong 12.6 \text{ kcal/(mole Å) and}$$

$$V_{X\ 1/2}(R_e' = 3.09\ \text{Å}) \simeq 1.7 \text{ kcal/mole.}$$

Less precise information was obtained by Golde and Kvaran[17] on the I 3/2 curve, because of unseparable emission overlaps in the II 3/2 → I 3/2 system. The I 3/2 curve was found to be slightly more repulsive than the X 1/2, the best fit values are:

$$-(dV_{I\ 3/2}/dR)_{R_e' = 3.09\ \text{Å}} \cong 29 \text{ kcal/mole/Å}$$

and

$$V_{I\ 3/2}(R_e' = 3.09\ \text{Å}) \cong 7.4\ \text{kcal/mole}.$$

Our best fit results give:

$$-(dV_{I\ 3/2}/dR)_{R_e'} = 28\ \text{kcal/mole/Å}$$

and

$$V_{I\ 3/2}(R_e' = 3.09) \cong 4.8\ \text{kcal/mole} \quad .$$

Thus, a comparison of the repulsive walls for the $V_{X\ 1/2}$ and $V_{I\ 3/2}$ reported in Table II and depicted in Fig. 7 with those determined from the spectroscopic study[17] shows good accord for the slopes of the curves and a satisfactory accord for the absolute positions. Although the spectroscopic estimate of $V_{X\ 1/2,I\ 3/2}(R_e')$ falls within the limits of our uncertainties (see Sect. III) for the Br-Ar potentials, we note that a perfect accord would be obtained if R_e' was taken to be 2.93 Å, which is 0.11 Å larger than R_e of KBr (2.82 Å).

An interesting result of Ref. 17 was the need to invoke van der Waals minima in the X 1/2 and I 3/2 states of Br-Ar in order to satisfy the upper limit for the electronic energy of the III 1/2 (B) state, as derived from the temperature dependence of the spectra. Our work provides also the necessary information on the relative energies of the X 1/2 and I 3/2 states in the well region. As discussed by

Golde and Kvaran, another way to satisfy the upper limit of the III 1/2 state is to lower the energy of it by changing R_e' towards smaller values, as suggested by our results. The emission spectra of Br-Kr has also been recorded, but no analysis has been yet reported.[4,16] Similar features as for Br-Ar were observed.

C. Recombination Studies.

Among the termolecular recombination processes of halogen atoms in the presence of a third body, those of bromine atoms in a rare gas environment have been studied most extensively, both experimentally and theoretically.[51] In general, the lack of detailed information on the halogen-rare gas interaction potentials made it difficult to evaluate the theoretical understanding of the termolecular recombination processes.[19-21]

Clarke and Burns[19b] computed rate constants for the recombination of bromine atoms in the presence of He, Ar and Xe by 3-D classical trajectory methods. They found that the radical molecules complex (RMC) mechanism was dominant for Ar and Xe at low temperatures; fairly good agreement between experiment and theory was obtained. A critical parameter in their model was the well depth of the Br-RG potential. Since the equilibrium constant for the process Br + 2 RG $\rightleftharpoons$ Br-RG + RG increases approximately exponentially with ϵ_{Br-RG}, the rate constant for the RMC recombination was significantly affected by ϵ_{Br-RG}. In their study, the interaction potential between Br and RG was assumed to be of the Lennard-Jones (L-J) form with the following parameters: RG=Ar, ϵ=1.0 kcal/mole, σ=3.0 Å; RG=Xe, ϵ=1.0 kcal/mole, σ=3.5 Å. A slightly shallower Br-Ar potential represented by a Morse function

(D_e=0.865 kcal/mole, r_e=3.51 Å) was used in another calculation.[19c] When the parameters of the Br-Ar potential were treated as adjustable constants in the phase space theory,[19c] better agreement with experiment was obtained. The optimum parameters were D_e=1.26 kcal/mole, r_e=2.4 Å. No reliable information was available then to indicate which set of parameters would better represent the Br-Ar potential.

The ϵ_{Br-Ar} was lowered to 0.5 kcal/mole in a study[19e] where the recombination path via unstable Br-Ar quasidimers was included in the calculations. Rate constants in agreement with experiment within a factor of 2 were obtained. It was noted that it would have been possible to obtain the negative temperature coefficient of the rate constant, in agreement with experiment, by choosing the proper ϵ_{Br-Ar}.

Most recent calculations[19f] made use of preliminary information from molecular beam data to better define the potential energy surface of the recombination process. By using the classical 3-D trajectory method with an improved sampling technique, reasonable agreement between computed and experimental rate constants was obtained for the Br recombination in He, Ar and Xe. The following L-J parameters were used for the Br-RG potentials: RG=He, ϵ=0.15 kcal/mole, σ=2.88 Å; RG=Ar, ϵ=0.6 kcal/mole, σ=3.32 Å; RG=Xe, ϵ=0.7 kcal/mole, σ=3.62 Å.

It should be noted that in all the theoretical recombination studies, the halogen-rare gas interaction has always been described in terms of a single potential energy curve. However, the effect of multiple potential curves or surfaces in systems containing open shell atoms needs careful consideration.[52]

V. CONCLUDING REMARKS

The experiments reported in this paper represent a further step towards the characterization of the ground state RG-X potential energy curves. Information unattainable by other techniques has been provided. A comparison between theory and experiment shows the existence of discrepancies in the predicted properties of both the excited and ground states of these molecules. In light of the many factors which may determine the peculiar RG-X electronic structure and which are not easily handled by the current theoretical treatment, these discrepancies are not surprising. An accurate knowledge of the ground state potential manifold, as derived from crossed molecular beam experiments, may serve the useful purpose of furnishing a reference for refining the excited state potentials in the theoretical simulation of emission spectra. It should be noted that there exists quite a good agreement between the slopes of the ground state potential estimated from diffuse spectra simulation and those derived from the experiments described in this paper. What our study adds is the absolute scale of the internuclear distance. Thus, the minimum positions and shapes of the excited states can be more reliably derived and more useful comparison made with the ground state alkali halide electronic structure and theoretical predictions. A fruitful "coupling" with spectroscopic techniques[53] and theoretical calculations should contribute to a more complete understanding of the RG-X electronic structure.

The investigation of the I-RG system is now underway,[50] which will complete the matrix of our scattering studies on the rare gas-halogen diatomic molecules. From the analysis of rows and columns of this matrix, the effect of the halogen and/or rare gas will be more fully discussed and the subtle transitions from van der Waals forces to chemical forces more clearly examined.

ACKNOWLEDGMENTS

P. C. wishes to thank Dr. Christopher H. Becker for many enjoyable and useful discussions. This work was supported by the Office of Naval Research (Contract No. N00014-77-C-0101), and by the Director, Office of Energy Research, Office of Basic Energy Sciences, Chemical Sciences Division of the U.S. Department of Energy under Contract Number W-7405-ENG-48. P.C. ackowledges a fellowship from the Italian Ministry of Education and travel support from NATO Grant No. 1444.

REFERENCES AND FOOTNOTES

1. For emission see e.g., (a) L. A. Kuznetsova, Y Y. Kuzyakov, V. A. Shpanskii, and V. M. Khutoretskii, Vestn. Mosk. Univ. Ser. II Khim. 19, 19 (1964); (b) M. F. Golde and B. A. Thrush, Chem. Phys. Lett. 29, 486 (1974); (c) J. E. Velazco and D. W. Setser, J. Chem. Phys. 62, 1990 (1975); (d) J. J. Ewing and C. A. Brau, Phys. Rev. A12, 129 (1975); (e) J. Tellighuisen, A. K. Hays, J. M. Hoffman, and G. C. Tisone, J. Chem. Phys. 65, 4473 (1976).

2. For laser action, see e.g., (a) S. K. Searles and G. A. Hart, Appl. Phys. Lett. 27, 243 (1975); (b) J. J. Ewing and C. A. Brau, Appl. Phys. Lett. 27, 350 (1975); (c) J. A. Mangano and J. H. Jacob, Appl. Phys. Lett. 27, 495 (1975); (d) G. C. Tisone, A. K. Hays, and J. M. Hoffman,, Opt. Commun. 15, 188 (1975); (e) C. A. Brau and J. J. Ewing, Appl. Phys. Lett. 27, 435 (1975); (f) J. M. Hoffman, A. K. Hays, and G. C. Tisone, Appl. Phys. Lett. 28, 538 (1976); (g) J. R. Murray and H. T. Powell, Appl. Phys. Lett. 29, 252 (1976); (h) J. G. Eden and S. K. Searles, Appl. Phys. Lett. 29, 350 (1976).

3. (a) T. H. Dunning and P. J. Hay, J. Chem. Phys. 69, 134 (1978); (b) P. J. Hay and T. H. Dunning, J. Chem. Phys. 69, 2209 (1978); (c) M. Krauss, J. Chem. Phys. 29, 350 (1976).

4. M. F. Golde, J. Mol. Spectr. 58, 261 (1975).

5. C. A. Brau and J. J. Ewing, J. Chem. Phys. 63, 4640 (1975).

6. J. Tellinghuisen, P. C. Tellinghuisen, J. A. Coxon, J. E. Velazco, and D. W. Setser, J. Chem. Phys. 68, 5187 (1978).

7. A. L. Smith and P. C. Kobrinsky, J. Mol. Spectr. 69, 1 (1978).

8. C. H. Becker, P. Casavecchia, and Y. T. Lee, J. Chem. Phys. 69, 2377 (1978).

9. A. Sur, A. K. Hui, and J. Tellinghuisen, J. Mol. Spectr. 74, 465 (1979). J. Tellinghuisen, J. M. Hoffman, G. C. Tisone, and A. K. Hays, J. Chem. Phys. 64, 2484 (1976).

10. C. H. Becker, J. J. Valentini, P. Casavecchia, S. J. Sibener and Y. T. Lee, Chem. Phys. Lett. 61, 1 (1979).

11. See, for example: P. J. Hay, W. R. Wadt, and T. H. Dunning, Ann. Rev. Phys. Chem. 30, 311 (1979), and references cited therein.

12. See: J. Tellinghuisen and M. R. McKeever, Chem. Phys. Lett. 72, 94 (1980), and references cited therein.

13. W. Kutzelnigg, Faraday Disc. Chem. Soc. 62, 185 (1977).

14. R. B. Bernsten and J. T. Muckerman, Adv. Chem. Phys. 12, 389 (1967); Ch. Schlier, Ann. Rev. Phys. Chem. 20, 191 (1969); U. Buck, Adv. Chem. Phys. 30, 313 (1975); H. Pauly, in Atom-Molecule Collision Theory, Ed. R. B. Bernstein (Plenum Press, New York, 1979), Chapter 4.

15. C. H. Becker, P. Casavecchia and Y. T. Lee, J. Chem. Phys. 70, 2986 (1979).

16. M. P. Casassa, M. F. Golde and A. Kvaran, Chem. Phys. Lett. 59, 51 (1978).

17. M. F. Golde and A. Kvaran, J. Chem. Phys. 72, 434 (1980); J. Chem. Phys. 72, 442 (1980).

18. J. Tellinguisen, A. K. Hays, J. M. Hoffman and G. C. Tisone, J. Chem. Phys. 65, 4473 (1976).

19. (a) A. G. Clarke and G. Burns, J. Chem. Phys. 55, 4717 (1971); (b) A. G. Clarke and G. Burns, J. Chem. Phys. 56, 4636 (1972); (c) V. H. Shui, J. P. Appleton, and J. C. Keck, Proc. 13th Symp. Combust. 1970 (1971), p. 21; (d) A. G. Clarke and G. Burns, J. Chem. Phys. 58, 1908 (1973); (e) W. H. Wong and G. Burns, J. Chem. Phys. 59, 2974 (1973); (f) D. T. Chang and G. Burns, Can. J. Chem. 54, 1535 (1976).

20. For some different viewpoints on theories of termolecular recombination, see also, G. Porter and J. A. Smith, Nature 184, 446 (1959); J. C. Keck, Adv. Chem. Phys. 13, 85 (1967); D. L. Bunker, Theory of Elementary Gas Reaction Rates (Pergamon, Oxford, 1966), Chapter 4; W. H. Wong and G. Burns, J. Chem. Phys. 58, 4459 (1973); and E. E. Nikitin, Theory of Elementary Atomic and Molecular Processes in Gases (Clarendon Press, Oxford, 1974), Chapter 7.

21. R. K. Boyd and G. Burns, J. Phys. Chem. 83, 88 (1979).

22. R. K. Sparks, Ph.D. Thesis, University of California, Berkeley, California, 1979.

23. Y. T. Lee, J. D. McDonald, P. R. Le Breton and D. R. Herschbach, Rev. Sci. Instr. 40, 1402 (1969).

24. J. J. Valentini, M. J. Coggiola, and Y. T. Lee, Rev. Sci. Instr. 48, 58 (1977).

25. C. H. Becker, P. Casavecchia, Y. T. Lee, R. E Olson, and W. A. Lester, Jr., J. Chem. Phys. 70, 5477 (1979).

26. See, e.g., E.H.S. Burhop, in Quantum Theory, D. R. Bates, editor (Academic Press, New York, 1961), Vol. I, Ch. 9.

27. V. Aquilanti and G. Grossi, J. Chem. Phys. 73, 1165 (1980).

28. V. Aquilanti, P. Casavecchia, G. Grossi and A. Lagana, J. Chem Phys. 73, 1173 (1980).

29. V. Aquilanti, E. Luzzatti, F. Pirani, and G. G. Volpi, J. Chem. Phys. 73, 1181 (1980).

30. R.H.G. Reid, J. Phys. B 8, L 493 (1975); R.H.G. Reid and R. F. Franklin, ibid. 11, 55 (1978); C. Harel, V. Lopez, R. McCarroll, A. Riera, and P. Wahnon, ibid. 11, 71 (1978); B. Amace and C. Bottcher, ibid. 11, 1249 (1978).

31. J. C. Slater and J. G. Kirkwood, Phys. Rev. 37, 682 (1931); see also K. S. Pitzer, Adv. Chem. Phys. 2, 59 (1959).

32. R. R. Teachout and R. T. Pack, At. Data 3, 195 (1971).

33. J. S. Cohen and R T. Pack, J. Chem. Phys. 61, 2372 (1974).

34. H. J. Werner and W. Meyer, Phys. Rev. A13, 13 (1976).

35. E. A. Reinsch and W. Meyer, Phys. Rev. A14, 915 (1976).

36. R. K. Preston, C. Sloane, and W. H. Miller, J. Chem. Phys. 60, 4961 (1974).

37. C. Froese Fisher, At. Data 4, 301 (1972). The quadrupole moment is obtained in terms of the mean value of $\langle r^2 \rangle$ over the valence orbital.

38. (a) C. H. Becker, R. J. Buss and Y. T. Lee, Materials and Molecular Research Division, Lawrence Berkeley Laboratory, University of California, Annual Report 1977 (LBL-7355), pp. 384-386; (b) See also, R. A. Aziz, J. Presley, U. Buck and J. Schleusener, J. Chem. Phys. 70, 4737 (1979).

39. J. A. Barker, R. O. Watts, J. K. Lee, T. P. Schafer and Y. T. Lee, J. Chem. Phys. 61, 3081 (1974).

40. C. H. Becker, R. J. Buss and Y. T. Lee, to be published.

41. See also, J. M. Farrar, T. P. Schafer and Y. T. Lee, AIP Conference Proceedings, No. 11, Transport Phenomena (1973), Ed. J. Kestin, p. 279.

42. R. J. Le Roy, Molecular Spectroscopy (The Chemical Society, London, 1973), Vol. I, pp. 113-176.

43. P. Brumer and M. Karplus, J. Chem. Phys. 58, 3903 (1973).

44. D. J. Ehrlich and R. M Osgood, Jr., J. Chem. Phys. 73, 3038 (1980).

45. M. Krauss and B. Liu, Chem. Phys. Lett. 44, 257 (1976).

46. B. Liu and A. D. McLean, J. Chem. Phys. 59, 4557 (1973).

47. Present work.

48. (a) D. Klingler, H. H. Nakano, D. L. Huestis, W. K. Bischel, R. M. Hill and C. K. Rhodes, Appl, Phys. Lett. 33, 39 (1978(; (b) J. H. Kolts and D. W. Setzer, J. Phys. Chem. 82, 1776 (1978); (c) H. C. Brashears and D. W. Setzer, Appl. Phys. Lett. 33, 821 (1978); (d) R. W. Waynant and J. G. Eden, IEEE J. Quantum Electron. 15, 61 (1979); (e) H. C. Brashears, Jr. and D. W. Setzer, J. Phys. Chem. 84, 224 (1980).

49. B. S. Ault and L. Andrews, J. Chem. Phys. 65, 4192 (1976).

50. P. Casavecchia, H. Guozhong, R. K. Sparks and Y. T. Lee, to be published.

51. For an up to date discussion on the current status of experiment and theory, see Ref. 21 and references cited therein.

52. D. G. Truhlar, J. Chem. Phys. 56, 3189 (1972); J. T. Muckerman and M. D. Newton, J. Chem. Phys. 56, 3191 (1972).

53. Also the laser induced fluorescence technique in supersonic free jets can yield useful information on the potential energy curves of the RG-X. See, for example: D. L. Monts, L. M. Ziurys, S. M. Beck, M. G. Liverman, and R. E. Smalley, J. Chem. Phys. 71, 4057 (1979).

Table I. Beam Characteristics and Center-of-Mass Collision Energies

Beam Br	Effective Temperature (°K)	Stagnation Pressure (Torr)	Mach Number	Peak Velocity (10^4 cm/s)	Δv/v (FWHM)	Average Collision Energies E (Kcal/mole) Br-Xe	Br-Kr	Br-Ar
9% Br_2 + 91% Xe	1206	700	8.1	7.86	0.17	4.2	3.8	2.9
7.7% Br_2 + 92.3% Ar	3017	820	10.5	12.42	0.15	9.8	8.4	-
6.3% Br_2 + 93.7% He	8505	1000	9.1	20.86	0.17	26.4	-	14.8
Xe	298	200	17.3	3.08	0.10			
Kr	296	300	17.6	3.81	0.10			
Ar	296	300	17.3	5.55	0.10			

Table II. Interaction Potential Parameters for Br-Ar, Kr, Xe, and Kr-Ar, Kr, Xe

System	Br-Ar		Br-Kr		Br-Xe		Kr-Ar	Kr-Kr		Kr-Xe
Electronic State	$X\frac{1}{2}$	$I\frac{3}{2}$	$X\frac{1}{2}$	$I\frac{3}{2}$	$X\frac{1}{2}$	$I\frac{3}{2}$	$1\Sigma^+$	$1\Sigma^+$		$1\Sigma^+$
ϵ (kcal/mole)	0.380	0.260	0.460	0.345	0.645	0.425	0.338[a]	0.394[b]	0.401[c]	0.465[d]
r_m (Å)	3.73	3.93	3.90	4.10	3.80	4.11	3.83	4.11	4.01	4.12
β_1	7.10	7.90	5.70	7.20	4.30	6.65	6.4	6.0		6.0
β_2	7.30	7.50	7.70	7.80	6.50	6.80	6.78	6.6		6.3
x_1	1.0255	1.0166	1.0231	1.0217	1.0405	1.0284	1.0118	1.1050		1.0289
x_2	1.700	1.700	1.700	1.600	2.000	1.900	1.45	1.60		1.37
C_6 (kcal/mole·Å^6)	1504.	1616.	2130.	2294.	3223.	3476.	1304.	1828.		2800.
C_8 (kcal/mole·Å^8)	8730.	8730.	13050.	13050.	21570.	21570.	7293.	10800.		15000.

[a] Ref. 38.
[b] Ref. 41.
[c] Ref. 39. This Kr-Kr potential should be more accurate than that of Ref. 41. Only ϵ and r_m are reported since the potential is not of the MMSV form. The repulsive walls are very similar.
[d] Ref. 40.

FIGURE CAPTIONS

Figure 1. Velocity distributions of bromine atom beams used on the experiments. Solid circles are from TOF data and lines are results of parametric fits to the deconvoluted distributions for the Mach numbers and temperatures given in Table I. Peaks are normalized to unity.

Figure 2. Laboratory angular distributions of scattered Br for the $Br(^2P) + Xe\ (^1S)$ system at three collision energies. Solid circles are data points and the solid curves are calculated from the best fit potentials of Table II, averaging over angular and velocity distributions of experimental conditions. Dashed and dashed-dotted curves represent the relative contribution to $I(\textcircled{H})$ of the X 1/2 and I 3/2 potentials of Table II, according to Eq. (1).

Figure 3. Laboratory angular distributions of scattered Br for the $Br(^2P) + Kr(^1S)$ system at two collision energies. Symbols are the same as in Fig. 2.

Figure 4. Laboratory angular distributions of scattered Br for the $Br(^2P) + Ar(^1S)$ system at two collision energies. Symbols are the same as in Fig. 2.

Figure 5. Interaction potentials for $Br(^2P_{3/2}) + Xe(^1S_0)$ obtained from experimental results shown in Fig. 2. Note the scale change at V(r) higher than 0.1 kcal/mole.

Figure 6. Interaction potentials for $Br(^2P_{3/2}) + Kr(^1S_0)$ obtained from experimental results shown in Fig. 3.

Figure 7. Interaction potentials for $Br(^2P_{3/2}) + Ar(^1S_0)$ obtained from experimental results shown in Fig. 4.

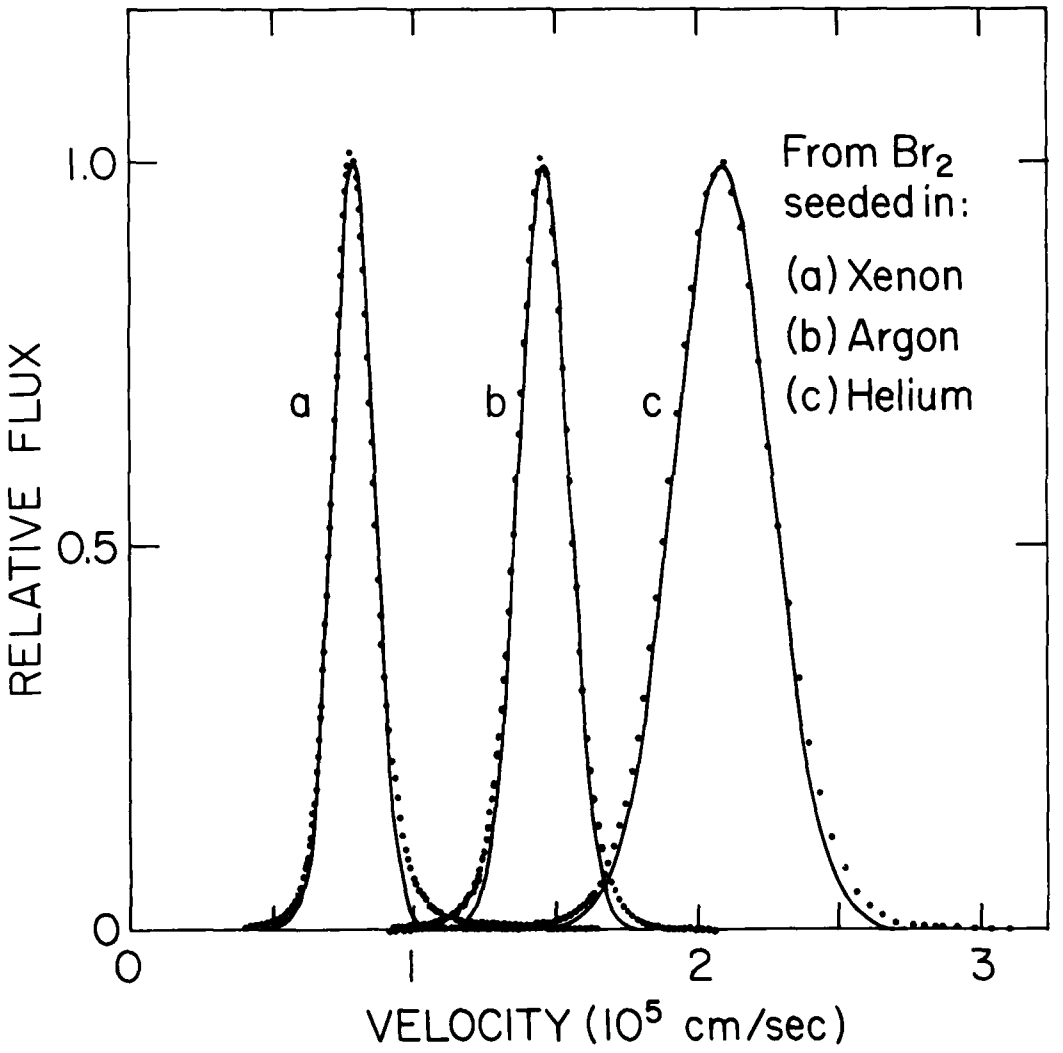

XBL 813-8456

Fig. 1

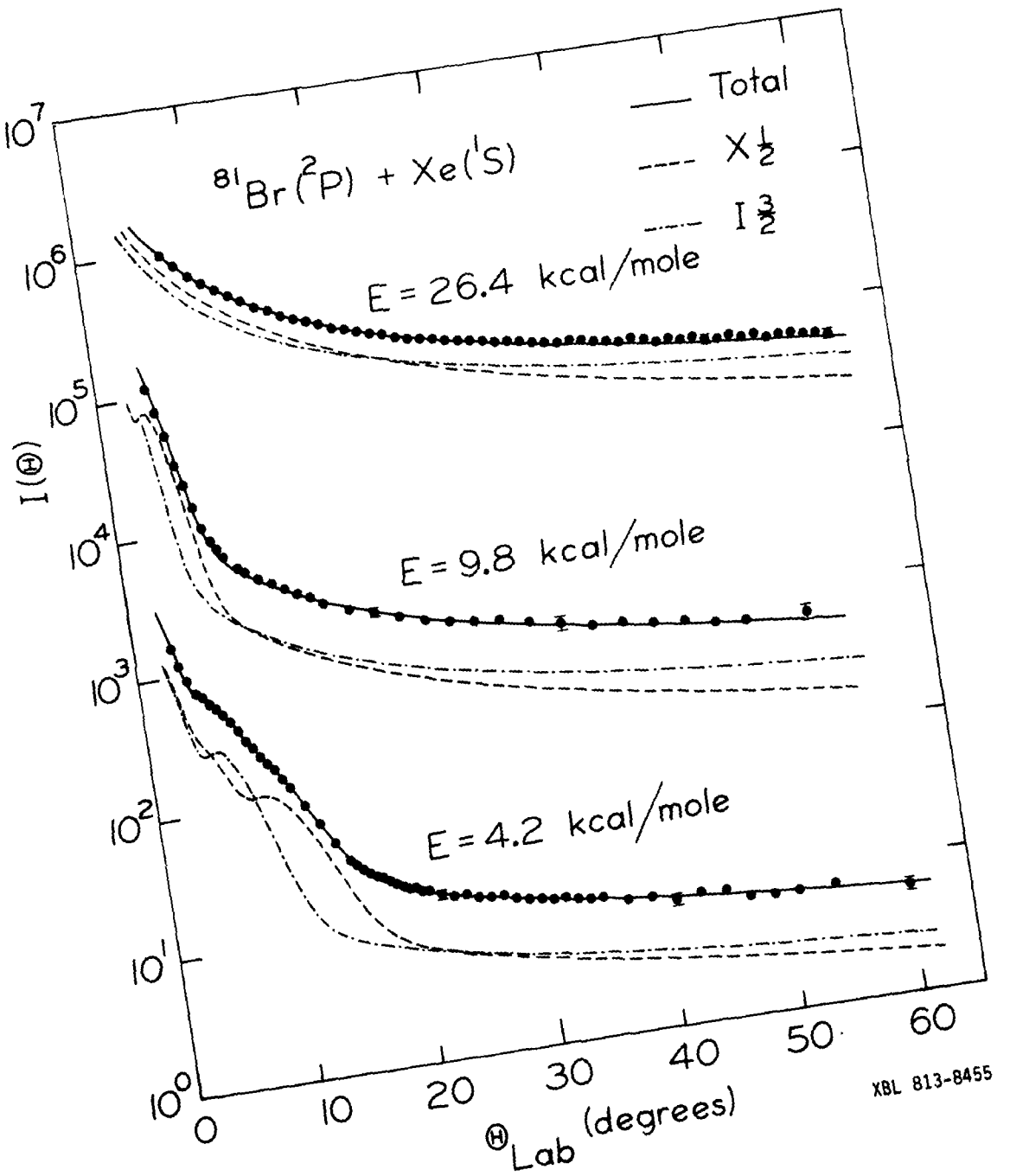
$^{81}Br(^2P) + Xe(^1S)$
Total
$X\frac{1}{2}$
$I\frac{3}{2}$
E = 26.4 kcal/mole
E = 9.8 kcal/mole
E = 4.2 kcal/mole
I(Θ)
10^7
10^6
10^5
10^4
10^3
10^2
10^1
10^0
0
10
20
30
40
50
60
Θ_{Lab} (degrees)
XBL 813-8455

Fig. 2

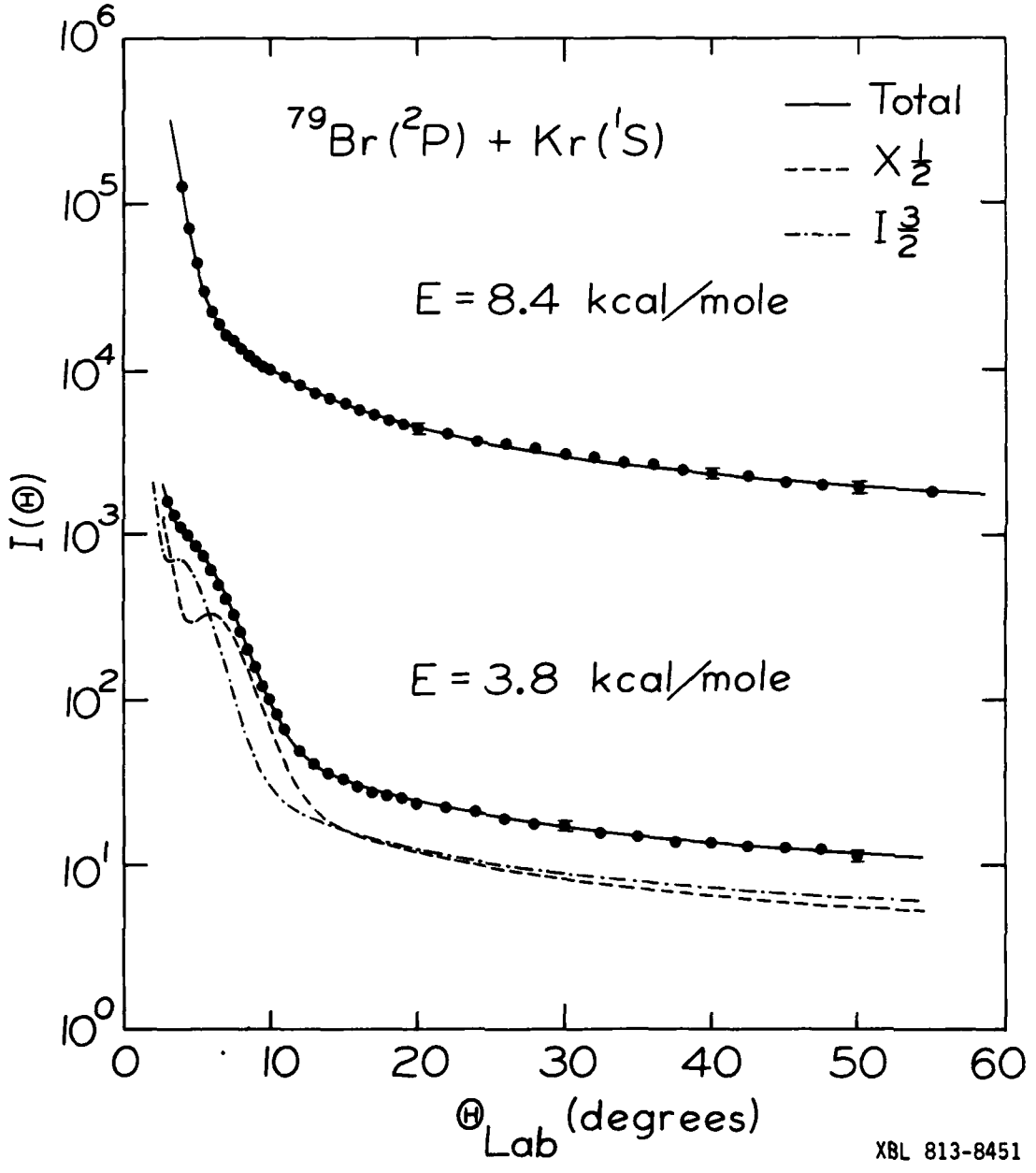
$^{79}Br(^2P) + Kr(^1S)$
Total
X 1/2
I 3/2
E = 8.4 kcal/mole
E = 3.8 kcal/mole
I(Θ)
10^6
10^5
10^4
10^3
10^2
10^1
10^0
0
10
20
30
40
50
60
Θ_{Lab} (degrees)
XBL 813-8451

Fig. 3

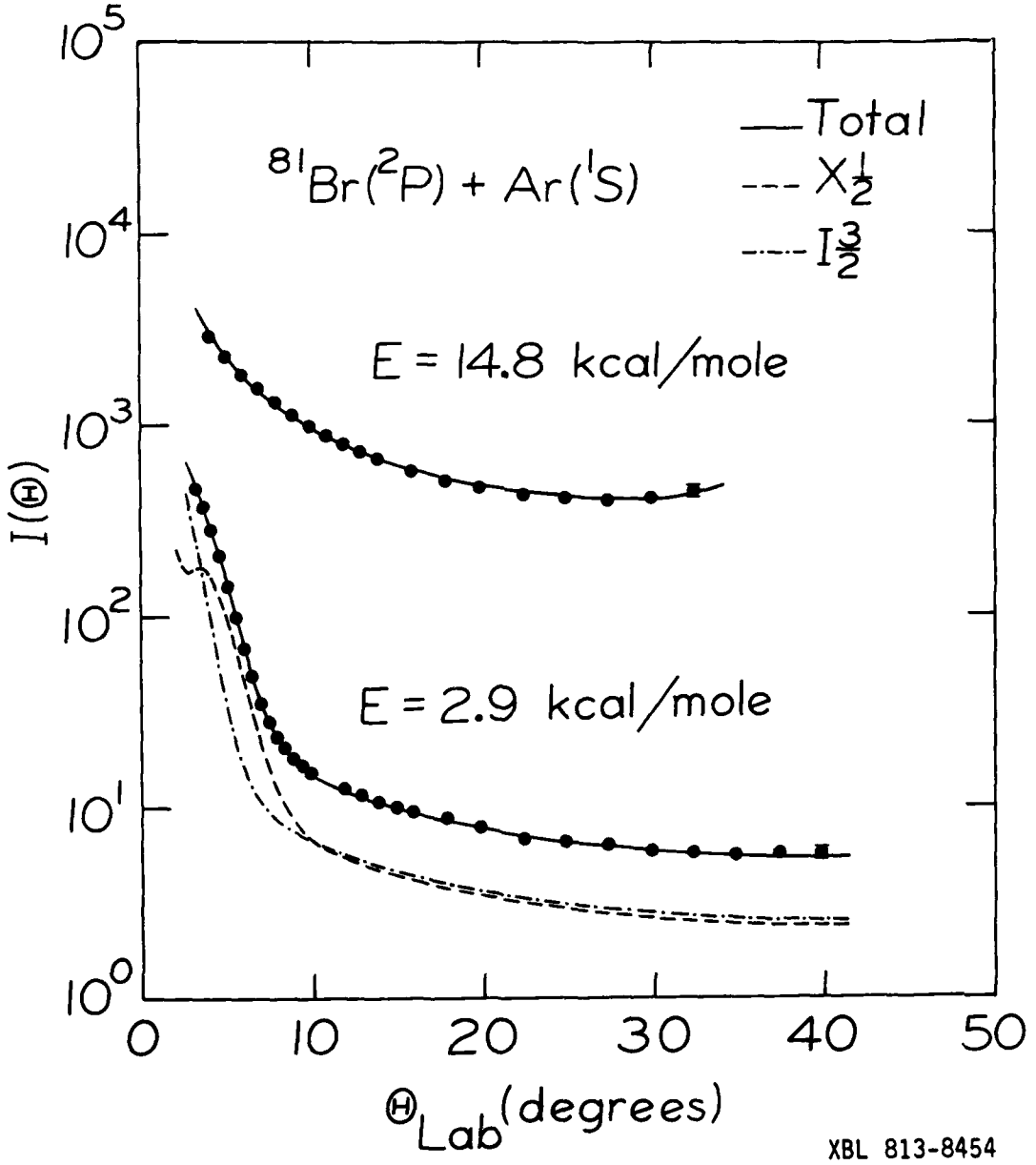
10^5
10^4
10^3
10^2
10^1
10^0
I(Θ)
$^{81}Br(^2P) + Ar(^1S)$
—Total
--- $X\frac{1}{2}$
-·-·- $I\frac{3}{2}$
E = 14.8 kcal/mole
E = 2.9 kcal/mole
0
10
20
30
40
50
Θ_{Lab}(degrees)
XBL 813-8454

Fig. 4

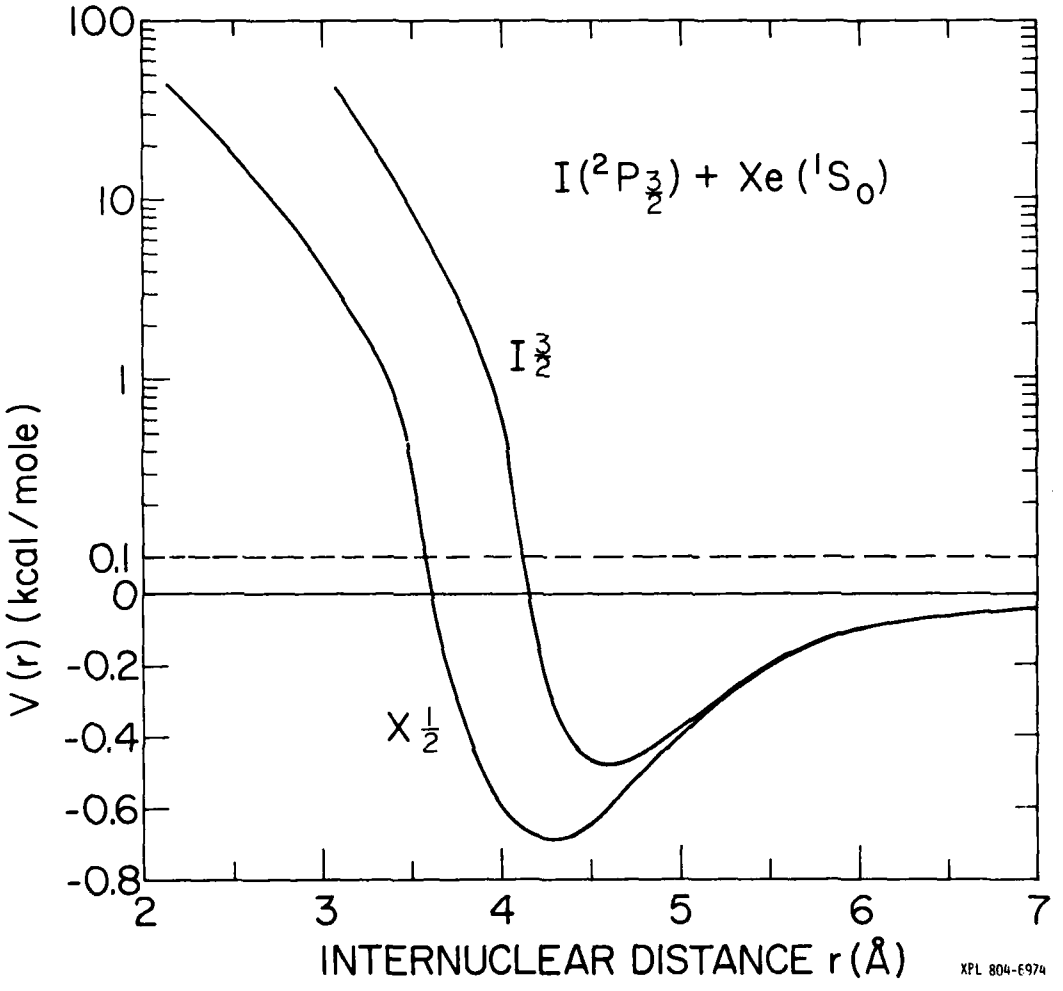
100
10
1
0.1
0
-0.2
-0.4
-0.6
-0.8
V(r) (kcal/mole)
2
3
4
5
6
7
INTERNUCLEAR DISTANCE r (Å)
$I(^2P_{\frac{3}{2}}) + Xe(^1S_0)$
$I^*_{\frac{3}{2}}$
$X_{\frac{1}{2}}$
XPL 804-6974

Fig. 5

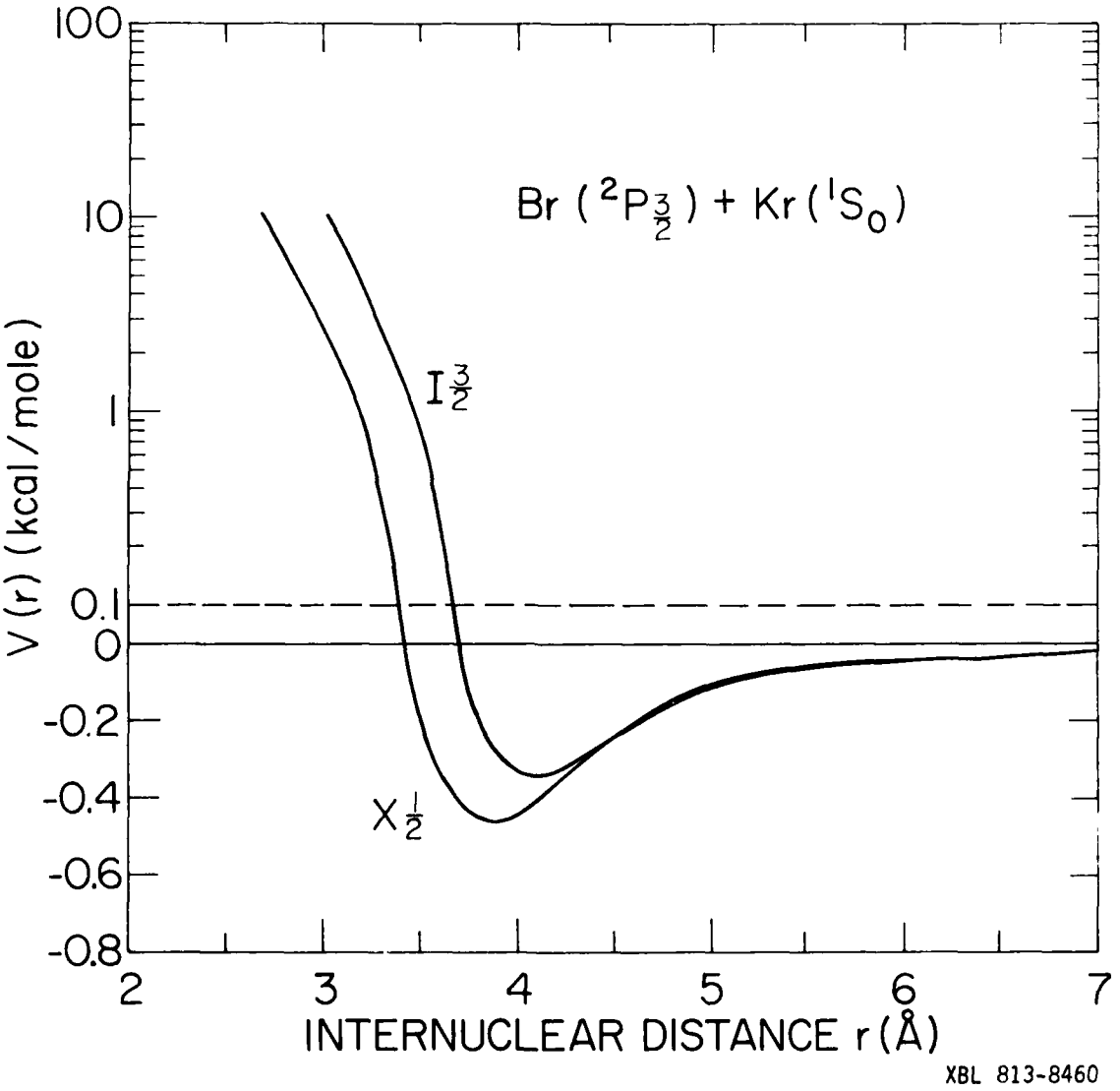
100
10
1
0.1
0
-0.2
-0.4
-0.6
-0.8
V (r) (kcal / mole)
Br ($^2P_{\frac{3}{2}}$) + Kr ($^1S_0$)
$I_{\frac{3}{2}}$
$X_{\frac{1}{2}}$
2
3
4
5
6
7
INTERNUCLEAR DISTANCE r (Å)
XBL 813-8460

Fig. 6

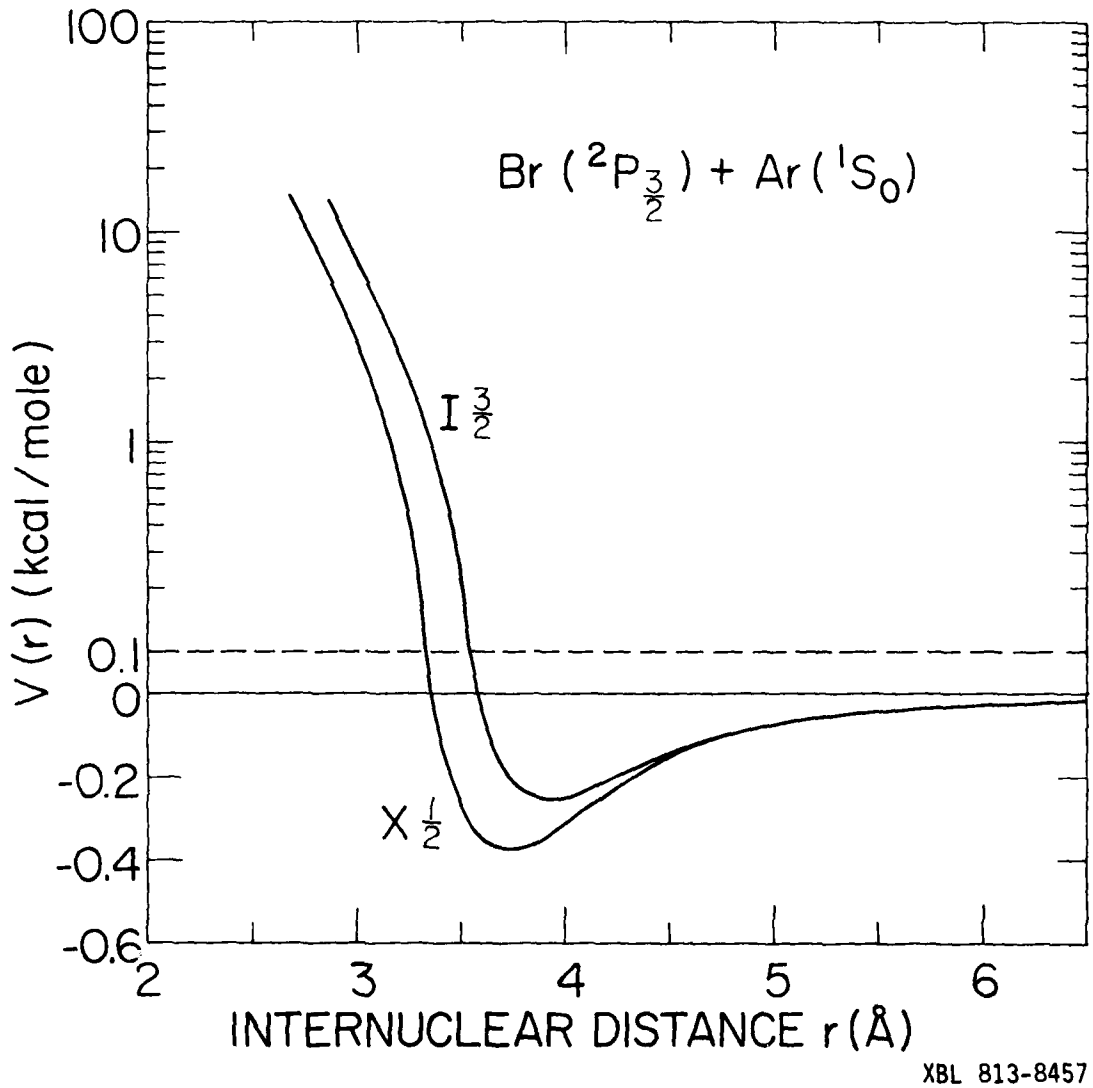
100
10
1
0.1
0
-0.2
-0.4
-0.6
V (r) (kcal / mole)
Br ($^2P_{\frac{3}{2}}$) + Ar ($^1S_0$)
$I_{\frac{3}{2}}$
$X_{\frac{1}{2}}$
2
3
4
5
6
INTERNUCLEAR DISTANCE r (Å)
XBL 813-8457

Fig. 7